Electronic Properties of Hybrid Organic/Inorganic Langmuir−Blodgett Films Containing CdS Quantum Particles

A. Samokhvalov,[†] Richard W. Gurney,[‡] M. Lahav,[‡] and R. Naaman*,[†]

Departments of Chemical Physics and Material and Interfaces, Weizmann Institute of Science, Rehovot 76100, Israel

Received: January 24, 2002; In Final Form: April 15, 2002

We investigated the electronic properties of hybrid inorganic/organic thin films where the inorganic components are monodisperse CdS quantum size particles (diameters 2.5 and 5 nm). For this purpose, low-energy photoelectron spectroscopy was applied in which the energy of photoelectrons, ejected from the metal substrate or from the films themselves, is measured. The electronic properties of hybrid Langmuir−Blodgett films were studied, when the films were deposited on gold or silicon surfaces and contained particles of different sizes arranged in layers at different distances from the substrate. For comparison films containing only the organic matrix were examined, so the effect of the quantum particles (QPs) on the electronic properties of the whole film could be resolved. The present study proves the importance of the organization of hybrid structure on its electronic properties. It is clearly demonstrated that the QPs cannot be considered as insolated species and that their electronic properties are affected by the structure of the film as a whole and by the substrate. It is shown that the QP size affects both the photoelectron emission yield and the scattering efficiency of electrons from the QPs.

Introduction

Semiconductor quantum particles (QPs) ranging in size from 1 to 10 nm continue to attract interest due to their unique electronic,[1−4] optical,[5−7] and catalytic[8,9] properties. The ability to control the size and organization of QPs in the form of superlattices has also been demonstrated.[10,11]

Hybrid inorganic/organic solids or thin films where the inorganic components are monodisperse metallic or semiconductor clusters of quantum size (diameter 1−10 nm) are of current interest due to their unique optoelectronic properties.[11,12] Any attempt to utilize QPs arranged within superlattices must consider the effects of the surroundings on the electronic properties of the QPs. Indeed, numerous studies on this subject have been performed using various methods including photoluminescence,[13,14] transient absorption,[15,16] transient excitonic bleaching,[17] valence-band photoemission,[18] and X-ray photoemission from the core levels of the QPs.[18,19]

Of particular interest are composite layers where the QPs are ordered into two entirely different length scales: a regular bonding geometry within each crystallite QP and the defined spacing between the QPs. Such materials should display functional cooperative properties that differ from the properties of each component.[20,21] For example, it has been reported that the photocurrent depends on the order of the QPs for the layer-by-layer hybrid films of CdS and ZnS QPs embedded in self-assembled monolayers.[22]

Here we investigated the electronic properties of hybrid LB films deposited on gold surfaces containing CdS QPs of different sizes arranged in layers at different distances from the substrate (Chart 1). For comparison, films containing only the organic matrix were studied, so the effect of the QPs on the electronic properties could be resolved.

CHART 1: Three Types of Hybrid Films That Were Investigated[a]

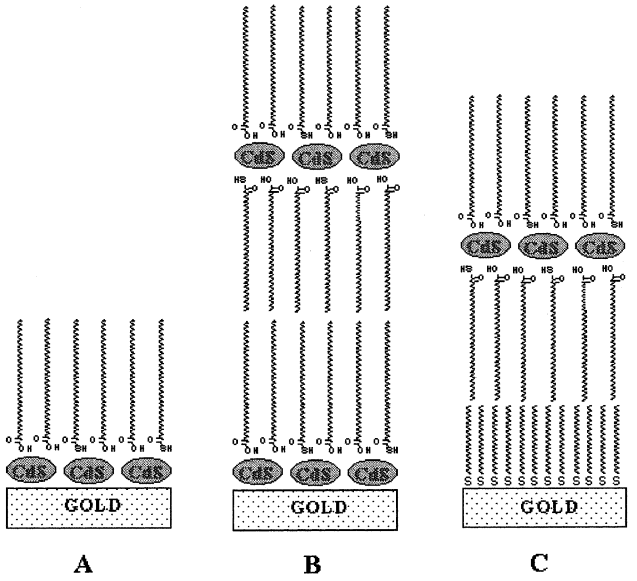

[a] The QPs could be deposited either directly on the substrate as a single layer (A), or in several layers, when the first is on the substrate (B). The film can contain layers with different particle sizes. A spacer could also be placed between the first layer and the substrate (C). In the precursor films of the relevant structure (before QP formation), Cd^{2+} ions are present instead of QPs.

The electronic properties of the films were investigated by low-energy photoelectron spectroscopy (LEPS)[23] in which the energy of photoelectrons ejected from the metal substrate was measured, after they were transmitted through the thin organic film. In previous studies, it had been proposed that the transmission of low-energy electrons through organized organic layers was governed by the film electronic band structure.[24−27]

[†] Department of Chemical Physics.
[‡] Department of Material and Interfaces.

10.1021/jp0202340 CCC: $22.00
Published on Web 08/13/2002

The first goal of our study is to identify what cooperative effects are influencing the electronic properties of the hybrid organic/inorganic structures, namely, how the electronic properties depend on the way the QPs are assembled as an organized structure and what the role of the organic matrix is. The second is to establish the role of the electronic interaction between the film and the substrate. The latter was accomplished by replacing the metal substrate by a semiconducting one, and by separating the metal substrate and the hybrid film with an insulating organic film ("spacer") of variable thickness.

Experimental Section

The details of the film preparation and characterization are given elsewhere.[28] Cadmium chloride (Aldrich), sodium sulfide (Aldrich), sulfuric acid (Merck), chloroform (Merck), ethanol (Merck), trifluoracetic acid (Merck), docosanoic acid ($CH_3(CH_2)_{20}$-COOH; Sigma), 1-heptanethiol (Aldrich), 1-dodecanethiol (Aldrich), and 1-octadecanthiol (Aldrich) were used without additional purification. The gold-coated glass slides (0.5 in. × 3 in. × 0.04 in. with 50 Å of titanium and 1000 Å of gold) were purchased from EMF Corp. (Ithaca, NY). The LB films for the XPS measurements were deposited on a silicon wafer coated with 50 Å of Ti, and then 1000 Å of Au. The (111) silicon wafer was B doped (p type) with a resistivity of 2−11 Ω·cm and thickness of 400−450 μm.

Preparation and Characterization of the Films. The organized hybrid organic/inorganic films comprised of QPs embedded within an organic matrix were prepared by applying a topotactic gas/solid reaction to Langmuir−Blodgett precursor films of Cd docosanoate/thiodocosanoate.[29] The presence of the thioalkanoate controls the site of QP nucleation within the Langmuir−Blodgett films, while its concentration within the mixed Cd alkanoate/thioalkanoate film determines the size of the QPs.

Mixed films of cadmium docosanoate and thiodocosanoate were prepared by Langmuir−Blodgett vertical dipping deposition of the monomolecular film from the aqueous subphase (target pressure 25 mN m^{-1}, dipping rate 10 mm min^{-1}, temperature 293 K, the number of layers varied) using a KSV Langmuir minitrough. The monomolecular films were prepared by spreading the mixed solution (99% chloroform/1% trifluoracetic acid) of the carboxylic and thiocarboxylic acids (90/10 and 50/50 ratios) on the aqueous subphase (1 mM solution of $CdCl_2$, pH 8.2). Immediately prior to deposition, the gold slides were cleaned in a Soxleth using toluene. Molecular layers of organic spacers of varying thickness were prepared on the gold surface either by self-assembly (thiols C_7 up to C_{18}) or by the Langmuir−Blodgett method (up to three bilayers of fatty acids $C_{20}CO_2H$). Prior to self-assembly, the gold slides were cleaned in a UVOCS chamber for 20 min and then washed for 20 min with absolute ethanol. Formation of the QPs inside the organic matrix was achieved by a topotactic gas/solid reaction of the LB films with the H_2S (from a commercial cylinder that was dried over $CaCl_2$ and $CaSO_4$ or generated in situ by reaction of Na_2S with 20% H_2SO_4), for 4 h at room temperature.

FT-IR spectra of the LB films were measured (1) on CaF_2 slides in transmission mode and (2) on films of gold in grazing incidence mode. UV−vis absorption spectra of the CdS QPs within the organic matrix were recorded in transmission mode on the Beckman DU-7500 spectrometer. The LB films with 20 layers of QPs were used for UV spectroscopy measurements. TEM images were taken on a Philips CM12 transmission electron microscope operated at 100 kV under low dose conditions, applying a CCD camera. LB films for these experiments were deposited on collodion/carbon-coated nylon grids (inert to H_2S) attached to glass slides for the dipping procedure.

XPS measurements were performed on a Kratos Analytical AXIS-HS instrument, using a monochromatized Al source at a relatively low power, 75 W, and a pass energy ranging between 20 and 80 eV.

SFM measurements were performed on a NT-MDT P47 scanning force microscope, using silicon cantilevers (NS611Ohm NT-MDT) with a resonance frequency of 120 kHz. Both the XPS and SFM studies and the results are described in detail elsewhere.[28]

LEPS Studies. The samples were attached to a holder and inserted into an ultrahigh vacuum chamber pumped to below 10^{-8} Torr. Details of the apparatus have been described elsewhere.[23] The kinetic energy distribution of the photoelectrons was measured by a time-of-flight (TOF) electron energy analyzer.

In the LEPS experiments, two types of lasers were applied. The first laser was used to emit photoelectrons from the sample: the excimer laser (Lambda Physik Compex 102) operating at 193 nm (single-photon photoemission mode). The second laser, Nd:Yag (Spectra-Physics), operating at its 3rd harmonics at 355 nm, was used to obtain two- or three-photon photoemission.

Results

Using the controlled surface charging (CSC) technique,[30] we were able to differentiate two different types of CdS QPs layers in the film. The two types differ in their respective distances from the Au substrate. There are QPs which interact strongly with the substrate and those that weakly interact. The first kind of QPs is formed when the layer of hybrid film is in direct contact with the substrate, and the second kind when the layer of hybrid film is about 3−4 nm or further from the substrate. The chemical composition obtained by XPS confirms, in principle, the expected structure for the films, before and after reaction with H_2S. The angular dependence of the signals substantiates the structure observed by SFM and is also consistent with the structure as presented in Chart 1.

The following experiment was performed to verify to what extent the QPs are in contact with the gold substrate. By using an organic solvent, the organic matrix can be dissolved and washed away. If the QPs of the bottom layer remain on the surface after washing, then they are covalently bound to it.

Films containing one layer of large QPs deposited on gold-coated glass slides were investigated. Before rinsing, the SFM shows uniformly arranged QPs with average dimensions of 5 × 5 × 0.5−0.8 nm. Swirling the film in a room temperature chloroform solution for 5 min dissolved the organic matrix. The film was dried with argon and immediately analyzed by SFM. After rinsing, SFM shows that the QPs remain on the surface. The size of the QPs increased due to coalescence; however, the QPs were not washed away with the organic matrix. These results suggest that the QP layer closest to the substrate may be in direct contact with the gold and perhaps is interacting covalently with the gold surface.

Single-Photon Photoemission with $\lambda = 193$ nm. The energy of the probe laser at 193 nm (6.42 eV), in the LEPS experiment, corresponds to the single-photon photoemission regime as demonstrated by the dependence of the total photoemission signal on the probe laser intensity. As the matrix and the spacer molecules are not photoionized, because their ionization potential (∼10 eV) is well above the probe photon energy, only the photoemission from the substrate and QPs of CdS needs to

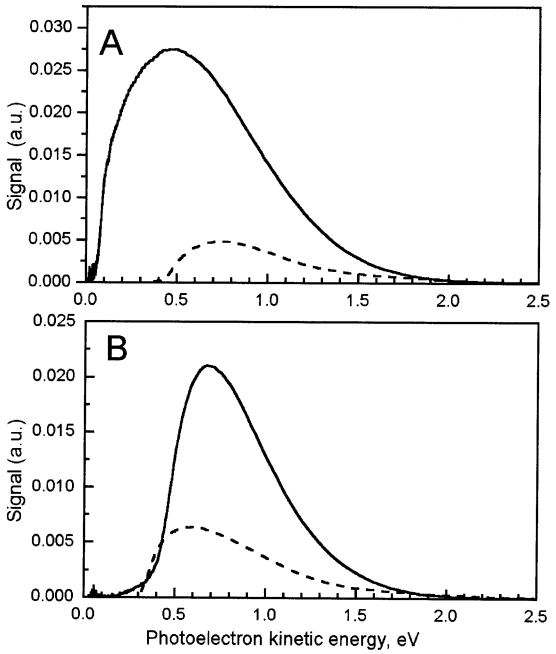

Figure 1. Photoelectron energy distribution when the photon energy is 6.4 eV ($\lambda = 193$ nm). The solid lines are the LEPS spectra obtained with films containing six hybrid layers of large (A) or small (B) QPs, while the spectra for the films without the QPs are shown as dotted lines.

be considered. In what follows we describe the results obtained when trying to determine the source of the photoelectrons, namely, whether they are originating from the QPs or from the gold substrate.

The LEPS spectra for a six-layer film with or without large or small QPs (parts A and B, respectively) are compared in Figure 1. The photoemission from QP-containing films is much higher than from identical precursor films, suggesting the increased emission results from the QPs. While the spectral shapes of the small-QP film with and without the QPs are basically identical, the spectrum of the large-QP-containing film differs substantially from that of the precursor. The precursor spectrum is dominated by electrons with energy above 0.4 eV, while a strong low-energy component below 0.4 eV is observed upon introduction of QPs into the film. The difference observed may result from extensive inelastic scattering in large-QP-containing films or from better transmission probability for large QPs at these low energies.

Normalized spectra from films of one to four layers of small (Figure 2A) or large (Figure 2B) QPs suggest that with an increasing number of layers there is a concomitant decrease in the high-energy part of the spectrum (above 1.5 eV). Efficient transmission of middle-energy (0.5−1.2 eV) electrons through the film is observed regardless of the film thickness. Additionally, as the number of layers increases, low-energy electrons appear; however, there is a sharp cutoff at the low-energy region of the spectrum depending on the thickness of the film. These observations indicate that the low-energy electrons (0.1−0.3 eV) are due to a better transmission probability of low-energy electrons in films containing large QPs and not a result of inelastic scattering. If the latter was the case, the number of low-energy electrons would be expected to increase with the number of layers. Finally, in the case of films containing four layers of either large or small QPs, the high-energy tail is greatly reduced, suggesting that the contribution from electrons ejected from the substrate is effectively eliminated, and the total observed emission is primarily from electrons ejected directly from the QPs.

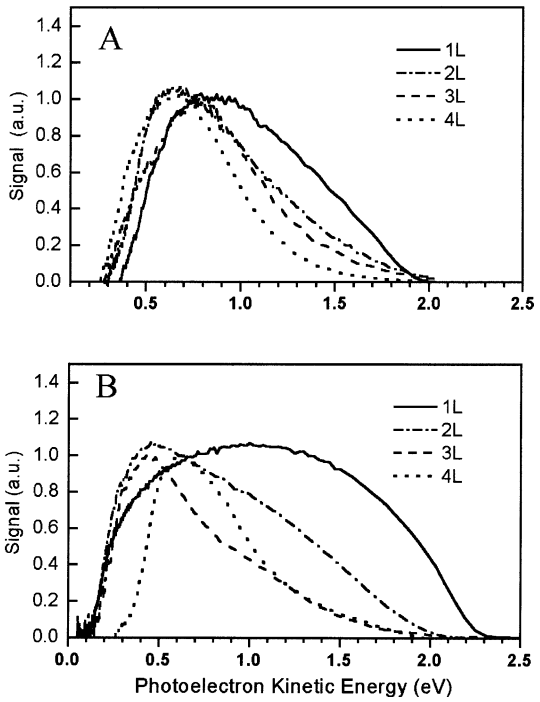

Figure 2. LEPS spectra obtained with 1−4 layers of small (A) or large (B) QPs ($h\nu = 6.4$ eV).

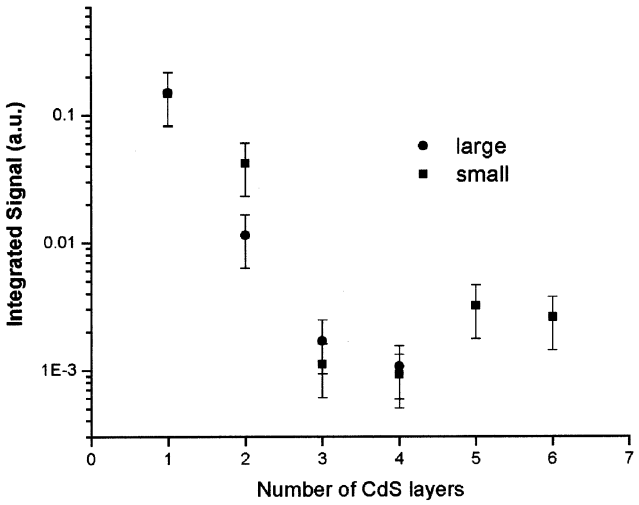

Figure 3. Integrated signal of photoelectrons measured as a function of the number of layers of large (circles) or small (squares) QPs ($h\nu = 6.4$ eV).

Figure 3 presents the integrated signal of electrons as a function of the number of layers. For samples containing up to three layers, the major contribution to the signal is from electrons ejected from the substrate. As a result, the decrease of the signal observed for one to four layers is due to scattering of electrons emitted from the substrate. The large QPs are more efficient scatterers than the small QPs, although the area covered by QPs, in both cases, is about the same. Since the integrated signal (IS) is the same for one layer of small and large QPs on gold, comparison between the IS of two layers of each, gives approximately the relative scattering probability of one layer of large QPs vs one layer of small QPs. In this analysis, we neglect the emission from the QPs themselves, which is a good approximation for a low number of layers (one to two layers) of QPs. Hence, on the basis of Figure 3, we conclude that the scattering of electrons by one layer of large QPs is by a factor of 5 more efficient than from one layer of small QPs. As will be discussed

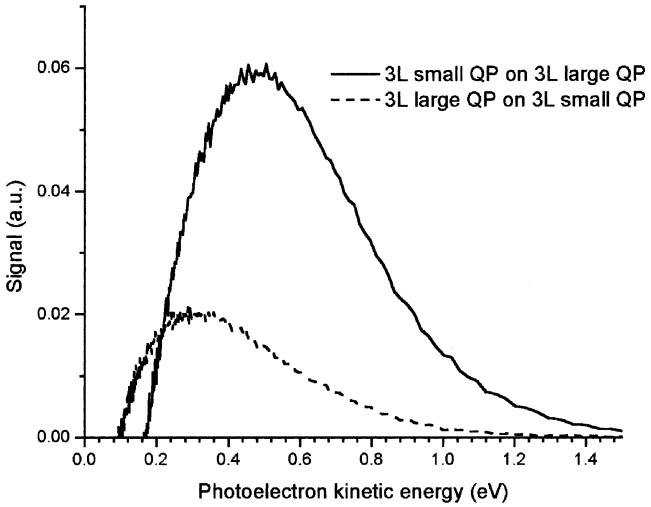

Figure 4. LEPS spectra obtained when three layers of large QPs are on top of three layers of small QPs (dotted line), and three layers of small QPs are on top of three layers of large QPs (solid line). The substrate in this case is an n-doped silicon wafer, and the photon energy is 6.4 eV.

below, this difference in scattering efficiency depends on the distance of the QPs from the substrate and the factor of 5 is valid when the QPs are about 3 nm away from the substrate.

As the number of layers increases beyond four, the signal is primarily comprised of electrons ejected from the QPs themselves. Therefore, the signal intensity is constant as the number of layers increases beyond four. The dependence of scattering on the size of the QPs can also be demonstrated by measuring the intensity of the LEPS signal for films having three layers of large QPs deposited above three layers of small QPs (on silicon) and vice versa. More efficient scattering of electrons by large QPs, as compared to the small QPs, is clearly demonstrated in the spectra in Figure 4. The intensity of the spectrum, where the large QPs are on the top, is clearly reduced compared to the opposite case, indicating the efficient scattering by the large QPs. The work function of silicon is higher than that of gold; therefore, the high-energy tail (>1.5 eV) is not observed here, confirming that indeed the high-energy (1−1.5 eV) tail in Figures 1 and 2 results from electrons emitted from the gold substrate.

As was discussed before, the low-energy cutoff in the LEPS is an indication for the band gap in the electronic structure of the film when an electron passes through it.[23,27] In Figure 4, the low-energy cutoff in the spectrum is almost the same for both types of films (small QPs on the large one and vice versa). This effect is different from the one observed for the same films deposited on gold[20] and demonstrates the importance of the substrate in defining the electronic structure of the film.

Figure 5 presents the LEPS spectra of a single layer of small QPs on top of three types of spacers, 7, 12, and 18 carbons long (parts A−C, respectively). For comparison the normalized emission from gold covered with the spacer alone is presented as a dashed line. The results indicate that the shapes of the spectra with and without the QPs are almost identical, indicating that the electron emission yield from the small QPs is small and that electrons emitted from the substrate control the spectra. The situation is very different when a layer of large QPs is used (Figure 6). By subtracting the LEPS spectra of the sample with the organic spacer only from the spectra with the QP-containing hybrid structure on top of the same spacer, the net contribution of the photoemission from the QPs is obtained (see the inset). While for the small QPs almost no such contribution exists,

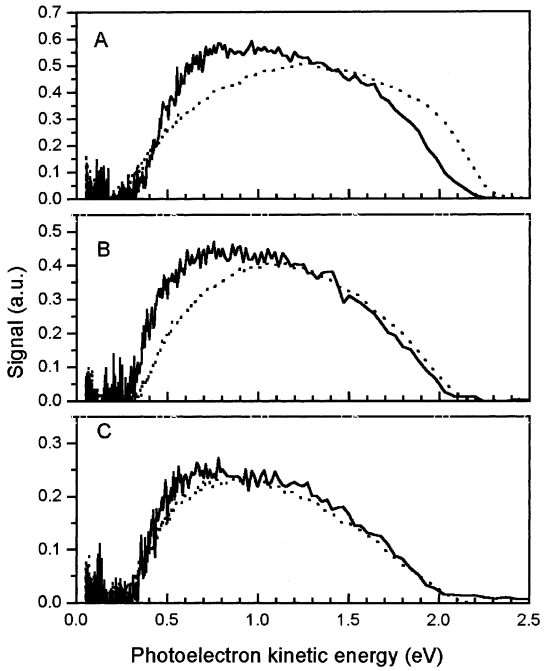

Figure 5. LEPS spectra of a single layer of small QPs on top of three types of spacers, 7, 12, and 18 carbons long (A−C, respectively). For comparison the normalized emission from the substrate covered with spacer only is presented as a dashed line ($h\nu = 6.4$ eV).

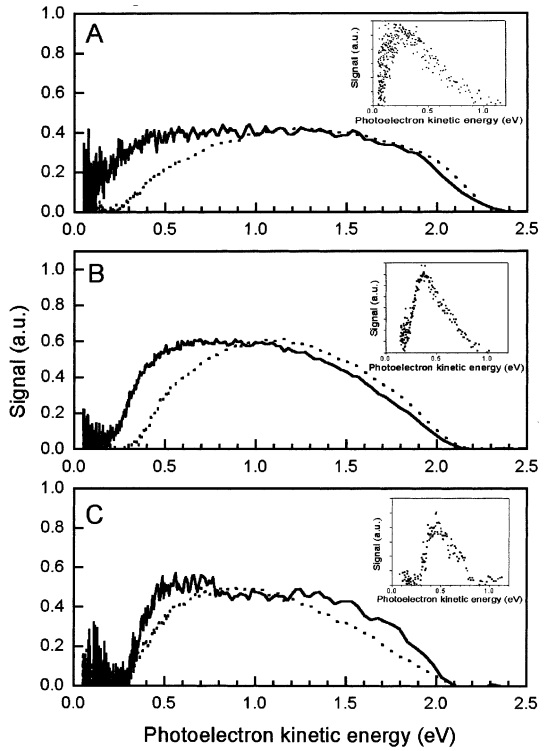

Figure 6. LEPS spectra of a single layer of large QPs on top of three types of spacers, 7, 12, and 18 carbons long (A−C, respectively). For comparison the normalized emission from the substrate covered with spacer only is shown as a dotted line ($h\nu = 6.4$ eV). By subtracting the spectra taken from the sample with the organic spacer only from that taken with the spacer and QPs on top of it, the net contribution of the photoemission from the QPs is obtained (see the insets).

the contribution from the large QPs is very distinct and clearly shows a peak at relatively low energy (0.5 eV).

It is interesting to compare the spectra from films of large QPs with different spacers. Clearly the spectrum of the short spacer film (inset in Figure 6A) is broader than that of the film

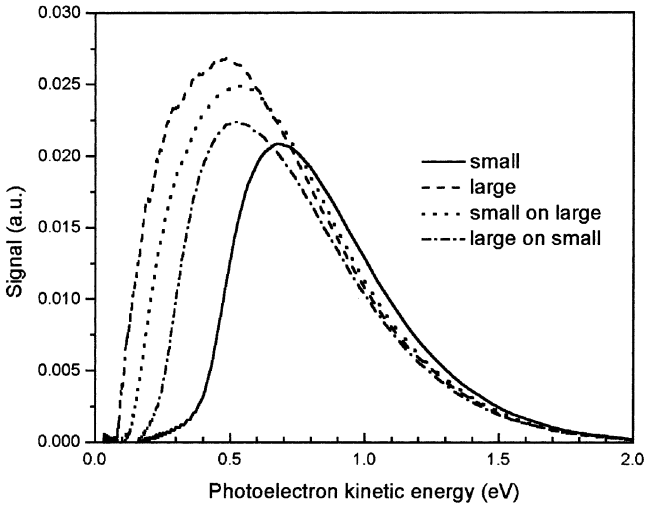

Figure 7. LEPS spectra taken with four types of films deposited on gold. Either six layers of small or large QPs or mixed films in which three layers of large QPs are deposited on three layers of small QPs or vice versa ($h\nu = 6.4$ eV).

with longer spacers. Hence, the metal substrate interacts with the QPs even when they are at a distance of about 1 nm. It is important to note that the subtraction spectrum shown in Figure 6C is similar to the subtraction spectrum of large QPs obtained in pump−probe experiments where the substrate contribution is eliminated.[20] In summary, the results indicate that scattering from large QPs is more efficient than from small QPs by a factor of 5 to 10.

The role of the metal substrate and film composition in determining the shape of the LEPS spectrum is demonstrated in Figure 7. Four types of films were studied: two films contained either six layers of small or large QPs, while two more were cascade-like films in which three layers of large QPs were deposited on three layers of small QPs or vice versa. It is evident that the low-energy cutoff in these spectra depends not only on the composition of the film but also on the order of the layer. The cutoff is different when large QPs are on top of the small QPs as compared to the reverse situation. The assignment of low-energy cutoffs to the cascade-like films "small on large" and "large on small" is exactly opposite for silicon and gold as substrate (Figure 7 vs Figure 4). The comparison between Figures 7 and 4 is indicative of the importance of the substrate in defining the properties of the film, as will be elaborated in the Discussion.

The results obtained with the 193 nm photons can be summarized as follows.

(1) The ionization potential of the QPs is less than 6.4 eV. As a result, depending on thickness of the film with QPs, the photoelectron spectrum is a mixture of electrons emitted from the substrate and from the QPs. When the film contains four layers of QPs or more, the emission from the QPs dominates the spectrum.

(2) The photoemission is more efficient from large QPs than small QPs.

(3) The scattering of electrons by the QPs depends on their size; larger QPs scatter electrons by about an order of magnitude more efficiently than the small QPs.

(4) The QPs interact with a metal substrate at a range of up to 2 nm. For a nonmetal substrate the interaction is much weaker.

Multiple-Photon Photoemission with $\lambda = 355$ nm. Figure 8 presents the LEPS spectra of a one-layer small QP film atop

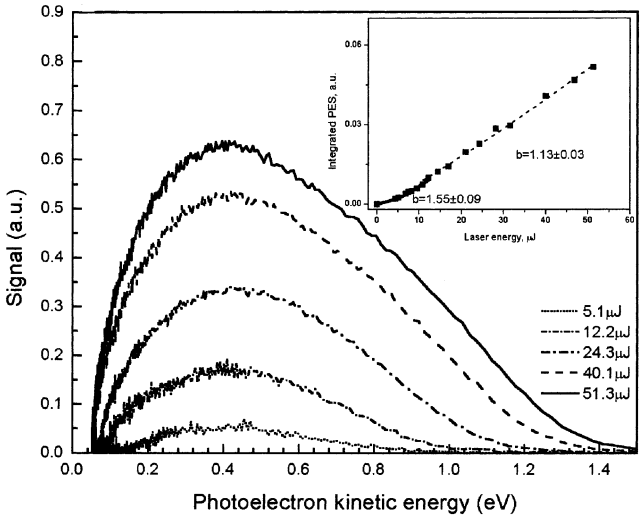

Figure 8. LEPS spectra obtained for one layer of small QPs placed on a spacer of seven carbons for different intensities of 355 nm photons ($h\nu = 3.5$ eV). In the inset, the power dependence of the integrated signal (squares) is shown fitted to the function $S = aI^b$, where I is the laser intensity and a and b are the two fitting parameters (dotted line).

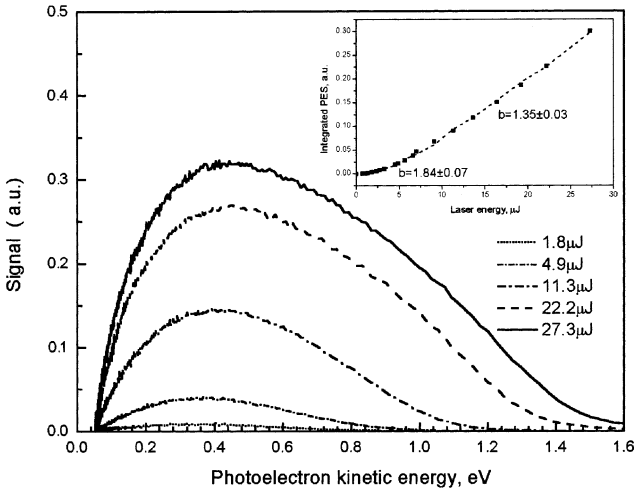

Figure 9. LEPS spectra obtained for one layer of large QPs placed on a spacer of seven carbons for different intensities of 355 nm photons ($h\nu = 3.5$ eV). In the inset, the power dependence of the integrated signal (squares) is shown fitted to the function $S = aI^b$, where I is the laser intensity and a and b are the two fitting parameters (dotted line).

a seven-carbon chain spacer for different intensities of 355 nm photons. In the inset, the power dependence of the integrated signal (S) is shown fitted to the function $S = aI^b$, where I is the laser intensity and a and b are the two fitting parameters. While for the low-energy range (up to about 13 μJ/pulse) the fitting can be performed with parameter $b \approx 1.5$, at the high-energy range, b is reduced to almost unity. Figure 9 presents the results obtained from a similar sample but this time with large QPs. In this case, for the low-intensity part of the intensity dependence $b \approx 1.8$ and it is again reduced for the high-intensity region to about 1.3.

The shapes and intensities of the LEPS spectra are similar for large and small QPs on the short seven-carbon spacer, except that large QPs show a higher energy tail (up to 1.4 eV for a laser intensity of 22 μJ compared to 1.2 eV for a laser intensity of 24 μJ for the small QPs) for the same laser energies. For comparison Figure 10 shows the intensity dependence of the LEPS spectra obtained with the short seven-carbon spacer with no QPs. Here, *the entire* intensity regime could be fitted with

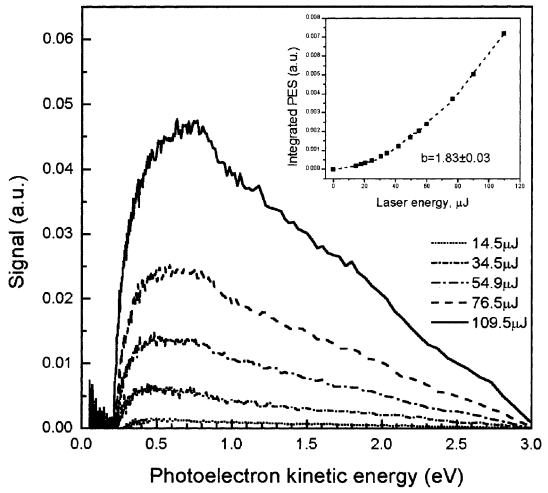

Figure 10. Intensity dependence of the LEPS spectra obtained with the substrate covered with the short seven-carbon spacer only with no QPs ($h\nu = 3.5$ eV). In the inset, the power dependence of the integrated signal (squares) is shown fitted to the function $S = aI^b$, where I is the laser intensity and a and b are the two fitting parameters (dotted line).

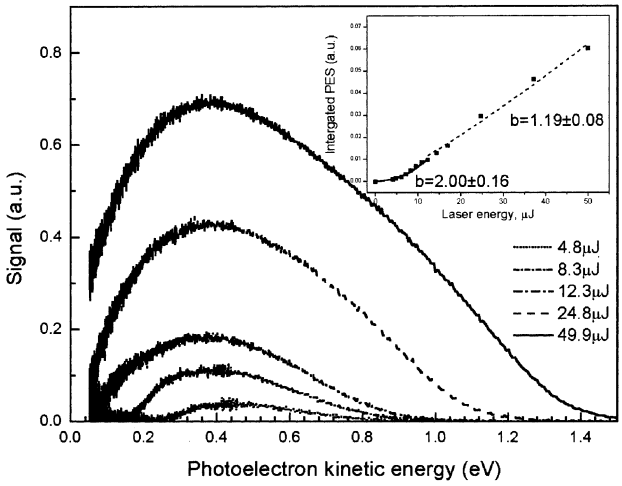

Figure 11. LEPS intensity-dependent spectra for small QPs deposited on a spacer 18 carbons long ($h\nu = 3.5$ eV). In the inset, the power dependence of the integrated signal (squares) is shown fitted to the function $S = aI^b$, where I is the laser intensity and a and b are the two fitting parameters (dotted line).

a single parameter, $b = 1.83$. It is also evident that much higher laser intensities are required for obtaining comparable electron emission. In addition, the spectra obtained with the spacer alone show a shoulder at the low-energy range (between 0.2 and 1.1 eV), which is not observable when the QPs are present.

Figures 11−13 show the LEPS intensity-dependent spectra for small, large, and no QPs, respectively, but this time with a spacer 18 carbons long. When the sample contains QPs (either large or small), the b parameter obtained for the low-intensity regime is about 2. At the high-intensity regime, it changes to about unity for the small QPs and the signal reaches saturation ($b < 1$) in the case of large QPs. When no QPs exist in the sample (the 18-carbon spacer only), b has a value of about 3, at the low-intensity region, that reduces to about 1.8 for the high-intensity regime. In addition, the total photoelectron signal is reduced significantly compared to that of the samples with the QPs. In Figure 13 the spectra have two regions. A relatively well-resolved narrow low-energy peak centered at ~0.4 eV and a broad high-energy tail extending up to above 2 eV. The laser intensity dependence for the low-energy peak fits b

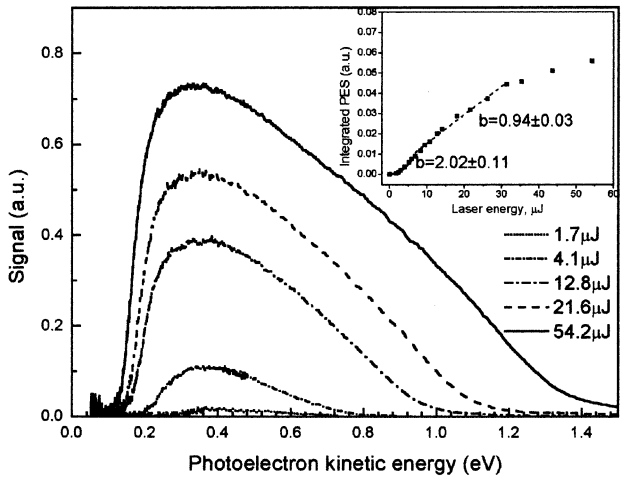

Figure 12. LEPS intensity-dependent spectra for large QPs deposited on a spacer 18 carbons long ($h\nu = 3.5$ eV). In the inset, the power dependence of the integrated signal (squares) is shown fitted to the function $S = aI^b$, where I is the laser intensity and a and b are the two fitting parameters (dotted line).

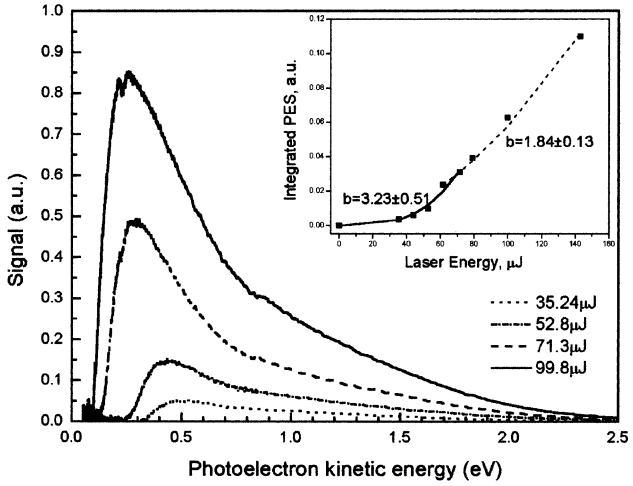

Figure 13. Intensity dependence of the LEPS spectra obtained with the substrate covered with the long 18-carbon spacer only with no QPs ($h\nu = 3.5$ eV). In the inset, the power dependence of the integrated signal (squares) is shown fitted to the function $S = aI^b$, where I is the laser intensity and a and b are the two fitting parameters (dotted line).

≈ 3, while for the broad high-energy tail $b \approx 2$. This means that two separate photoemission sources are present for the 18-carbon spacer on gold. All the data shown in Figures 8−13 are shown to scale, so that the emission yield can be compared directly.

In the case of a sample containing the precursor only, namely, no QPs (spectrum not shown), on top of the 18-carbon spacer, the intensity dependence can be fitted with a b of about 1.5 for all laser intensities and saturation is not observed, unlike the case when the films contain QPs. In addition the total emission is much lower compared to that of films of similar structure with QPs, implying direct photoemission from QPs.

When the photoelectron spectra of 7-carbon and 18-carbon spacers without QPs are compared, the following differences can be recognized: (a) The signal observed with the short spacer is smaller compared to that of the sample with the long one. (b) The sample with the short spacer does not show cubic intensity dependence. (c) The low-energy peak in the case of the short spacer is barely resolved, unlike in the case of the long one. From these results we can conclude that the low-energy peak in Figure 13 results from direct photoionization of

the chains by a multiple (three) photon process and that the broad background that is extended to high photoelectron energy is due to emission from the gold substrate. In the case of the short chains (seven carbons), almost no photoionization of the chains exists and the observed photoelectrons result from the gold substrate almost solely.

The results obtained with the 355 nm photons can be summarized as follows.

(1) In the case of samples with QPs, the power dependence reaches saturation ($b \leq 1$), while this effect is not observed for the samples that do not contain QPs (the spacer only or precursor on top of the spacer).

(2) The power dependence for the sample containing QPs depends on the spacer. With a spacer of 18 carbons, b at low intensities is about 2, becomes unity, and then shows saturation ($b < 1$). The power dependency of 2 and narrow LEPS band mean coherent two-photon photoemission from QPs on top of the 18-carbon spacer. For the seven-carbon-chain spacer, b is about 1.7 at low intensities and reduces to about 1.2 at the higher intensities.

(3) The photoemission from QPs in proximity (10 Å) to the substrate is affected by the substrate in the following ways: there is no difference in photoemission yield between the large and small QPs, and coherent two-photon emission from the CdS QPs cannot be detected.

(4) In general, when there are no QPs (precursor or spacer only), the signal is much lower compared to that of samples with the QPs.

(5) In the case of the 18-carbon spacer only, the cubic power dependence (fitting parameter $b \approx 3$) indicates a large contribution from direct ionization of the chains by three-photon photoemission. In the case of the shorter spacer (seven-carbon chain), there is less contribution to the signal from direct ionization of the organic molecules and $b < 3$.

(6) When small and large QPs on the 18-carbon spacer are compared at low laser intensity, the signal from the sample containing large QPs is 3 times stronger than that from the sample with small QPs (Figures 12 and 11, respectively). This is an indication of a higher quantum yield of photoemission from large QPs, as also observed in the case of excitation at 193 nm.

Discussion

The present study allows insight to be obtained into the photoemission properties of QPs, the electron−QP interactions, and the coupling between the different components of the hybrid film, namely, the QPs, the organic matrix, and the substrate. All these properties were characterized as a function of the QP size and their distance from the substrate.

By monitoring both large and small QPs, the quantum size effect on their properties was estimated. By changing the spacer length, the surface proximity effect was established, and by varying the laser excitation wavelength, it was possible to separate photoemission and scattering properties of the different elements in the film.

In what follows we will discuss separately the electron emission properties and the scattering properties.

Electron Emission. As already mentioned in the Results, in the single-photon mode, only the gold substrate and the QPs can contribute to the photoelectron signal. In trying to determine the ionization potential (IP) of the QPs, one must take into account their relatively broad size distribution.[20] As the subtraction LEPS spectra imply (Figure 6) the IP of the QPs is 6−6.4 eV. The subtracted LEPS spectra reflect the density of filled states in the QPs and are consistent with the density of states determined by the attenuated LEPS (ALEPS) spectra published before.[20]

The quantum yield of photoemission is higher for large QPs, meaning lower IP and higher density of states near its valence band edge, compared with small QPs. As shown below, in the multiple (two and three) photon photoemission mode it is possible to determine the exact IP and density of states of organic spacers and of the CdS component of the hybrid films.

The hydrocarbon chain of the long C_{18} spacer can be ionized by a coherent three-photon process, $3h\nu = 10.5$ eV (Figure 13), while shorter chains do not contribute to the three-photon photoemission. The relatively broad (fwhm $\approx$ 0.4 eV) well-resolved low-energy LEPS band (maximum at 0.5 eV) corresponds to ionization of the σ states of the alkyl C_{18} chain. Its IP is ~10 eV, and the binding energy (BE) is about 5 eV below the Fermi level. This band is well-known from UPS studies of long-chain (C_{16}) alkylthiol on Au(111).[31] It is assigned to the C−H band constituted by the molecular orbitals of C 2p and H 1s states. It is known from UPS studies that shorter alkyl chains have only a weak band corresponding to emission from the same state.[31] This is consistent with the lack of contribution of the short carbon spacers to the direct coherent three-photon ionization observed in the present work.

The QPs on top of the long C_{18} spacer show coherent two-photon photoemission ($b \approx 2$) (Figures 11 and 12), which is not found when the spacer is shorter. This coherent process is accompanied by a relatively narrow symmetric LEPS band shape (fwhm $\approx$ 0.4 eV). These results imply ionization of the valence states of the QPs, and the LEPS bandwidth manifests, most probably, the size distribution of the QPs. Hence, the ionization potential of QPs on the C_{18} spacer can be determined from the high-energy onset at the low-laser-intensity regime (laser energy 12 μJ/pulse) considering that $2h\nu = 6.98$ eV. The ionization potentials obtained are 6 and 6.2 eV, for the large and small QPs, respectively. These values are consistent with data obtained with the 193 nm light (6.4 eV), where an indication of direct single-photon photoemission from QPs was observed. These values of the IP also explain why the contribution to the photoemission is larger from the large QPs, since their ionization potential is lower.

The question is why no evidence for coherent two-photon photoemission can be observed from the QPs when the spacer is short (seven-carbon chain). It seems that the explanation for this is the strong coupling, in this case, between the QPs and the substrate. From Figure 6, we can estimate the range of the interaction between the substrate and the QPs, since we observe that the LEPS difference spectra keep changing with changing spacer length till about 1.5 nm (which correlates with the 12-carbon spacer). The nature of the effect is unlikely due to donor−acceptor interaction between the QPs and the substrate, since this coupling is typically of short range and because we observed no change in the work function upon deposition of the QPs on the spacer. This clearly proves that no charge transfer occurs. On the other hand, electrostatic (image charge) interaction can result in a long-range coupling, and it is expected to decay to an insignificant value over a range of about 2 nm. In the case of the dielectrics-coated metals, it has been shown that the image potential can extend over a relatively long distance.[32] For instance, in the case of a double layer of *n*-heptane on Ag, the image potential spans up to 20 Å away from the metal surface.[32]

As discussed above, photoemission from QPs that are not coupled with substrate (3 nm spacer or more) can be observed

by applying the 355 nm laser. The large QPs show a factor of 3 larger photoemission signal, and their IP is 200 meV lower than that of the small QPs. These differences can be explained by the quantum size effect, even though differences are blurred due to broad size distributions for both the large and small QPs. When the QPs are close (1 nm) to the substrate, the photoemission yield is independent of the particle size. This effect is consistent with the electrostatic coupling proposed above, which tends to equalize the ionization potentials of QPs near the metal substrate.

Scattering Properties. Following the electron emission, the transmission properties of the films determine the shape of the photoelectron spectrum. As was discussed before, low-energy electron transmission through organized organic films is controlled by the band structure in these films. As will be shown below, this is also the case for hybrid films that contain both QPs and an organic matrix. Specifically, here we will discuss the effect of the QP size on the band structure and the influence of the substrate on the band, a new feature that is not observed in regular organized organic films.

Since the size of the QPs was varied and the spectra were taken with and without QPs (with the organic matrix alone), in the present work it is possible to focus on the specific contribution of the QPs to the transmission properties of the film. Specifically, we intend to focus on the quantum size effect.

The results show clearly that the total electron transmission through films containing large QPs is lower than when the films contain small QPs. This means the large QPs scatter electrons more efficiently. This effect cannot be explained by coverage, because the relative surface coverage by the large QPs is similar to that of the small QPs, as is evident from TEM studies. Hence, the difference in efficiency must result from the electron affinity, which is expected to increase with the QP diameter and can cause more efficient trapping of electrons by the QPs.

Another manifestation of the quantum size effect is the band gap of the QPs. It is important to realize that the band gap manifests in the low-energy cutoff of the spectrum. Another important point is that we expect the band gap observed to be independent of the source of the electrons. Namely, if the electrons are ejected either from the substrate or from the QPs, their transmission through the film depends on the band gap as is clearly shown in Figure 1, where the low-energy cutoff moves to lower energy for the large QPs. This effect is observed also in Figure 7. While in Figure 7 the high-energy cutoff in the photoelectron spectra is identical for all four films, there are substantial differences in the low-energy cutoff for all those samples. The spectra of the only large or only small QPs were different, with low-energy "cutoffs" at 0.1 and 0.35 eV, respectively. The low-energy cutoff of the two "cascade-like" films (three layers of small QPs on top of three layers of large ones and vice versa) depends on which layer of the QPs is close to the gold. For the cascade-like structure with the large QPs residing on the bottom, the cutoff was at higher energy relative to the one with only large QPs. It was lower in energy relative to the cascade-like structure of the "opposite" sense of polarity with the small QPs being close to the gold.

Two important observations were made. The first is that the LEPS spectrum observed for films containing QPs of the two sizes is not a simple additive spectrum from each of the QPs. Specifically, the low-energy cutoff appears as a weighted average of the cutoffs obtained for the films containing one size of QPs only. The other observation is that if there are QPs near the metal substrate (no spacer), then their contribution to the weighted average is more significant than that of the QPs that are located farther away from the surface. This phenomenon can be explained by adapting the band-gap model to explain the low-energy cutoff. Hence, the question is how the band structure depends on the existence of QPs of different sizes. In our approach we shall follow the convention for calculating the band gap for alloys of semiconductors.[33] In such alloys the band gap is the weighted average of the band gaps of its components. This effect results from the dependence of the band gap on the average interaction between the atoms in the alloys. Namely, the band gap is given by $2\langle V\rangle$, where V is the interaction between the QPs. When QPs of different sizes are involved

$$\langle V\rangle = \sum_i \rho_i n_i V_i \Big/ \sum_i \rho_i n_i \tag{1}$$

where ρ_i and n_i are the density of states and fraction of the ith component, respectively. Typically, the density of states is similar in many semiconductors, and therefore the band gap depends only on the fraction of each component. However, in the case of no spacer, the lowest layer of the QPs can interact with the metal substrate via the image potential. This interaction decreases the ionization potential of those QPs and increases the effective density of states in the layer by broadening its states. Therefore, when the broadened state of the low-lying layer interacts with the other layers, its weight increases. In this case eq 1 can be approximated to be

$$\langle V\rangle = \frac{n_1\rho_1 V_1 + n_2(\rho_2 + \rho_M)V_2}{n_1\rho_1 + n_2(\rho_2 + \rho_M)} \tag{2}$$

where the indices 1 and 2 refer to the QPs on the top and those near the surface, respectively. The density of states of the low-lying layer that interacts with the density of states of the metal substrate, ρ_M, is more dominant in defining the band gap than expected on the basis of its fraction in the film.

Figure 4 supports our conclusion regarding the role of the metal substrate. In this case, the substrate is silicon and as a result no image−charge type interaction exists between the low-lying QPs and the substrate. Hence, the band gap observed is controlled actually by the upper layers, through which all the electrons have to pass. When the large QPs are on the top, because of the narrower band gap, typical of them, the low-energy cutoff is slightly at lower energy than in the opposite case.

The importance of the metal substrate in controlling the electron energy distribution and its long-range effect was already discussed above in relation to the ionization potential and the emission yield. The effect of the metal substrate on the band gap is another manifestation of the electrostatic interaction between the low-lying QPs and the metal.

Summary

We investigated the electronic properties of hybrid films that are composed of an organic matrix containing ordered quantum QPs by applying single- and multiple-photon low-energy photoelectron spectroscopy. The present study proves the importance of the organization of hybrid structure on its electronic properties. It is clearly demonstrated that one cannot relate to the QPs as isolated species and that their electronic properties are affected by the structure of the film as a whole and by the substrate. It has been shown that the quantum size affects both the photoelectron emission yield and the scattering efficiency of electrons from the QPs.

Acknowledgment. AS and RN acknowledge the partial support of the Israel Science Foundation.

References and Notes

(1) Henglein, A. *Chem. Rev*. **1989**, *89*, 1861.
(2) Steigerwald, M. L.; Brus, L. E. *Acc. Chem. Res*. **1990**, *23*, 183.
(3) Wang, Y.; Herron, N. *J. Phys. Chem*. **1991**, *95*, 525.
(4) Weller, H. *Angew. Chem., Int. Ed. Engl*. **1993**, *32*, 41.
(5) Wang, Y. *Acc. Chem. Res.* **1991**, *24*, 133.
(6) Rosencher, E.; Fiore, A.; Vinter, B.; Berger, V.; Bois, P.; Nagle, J. *Science* **1996**, *271*, 168.
(7) Hines, M. A.; Guyot-Sionnest, P. *J. Phys. Chem*. **1996**, *100*, 468.
(8) Bard, A. J. *Science* **1980**, *207*, 4427.
(9) Yanagida, S.; Yooshiya, M.; Shiragami, T.; Pac, C. J.; Mori, H.; Fujita, H. *J. Phys. Chem.* **1990**, *94*, 3104.
(10) (a) Heitmann, D.; Kotthaus, J. P. *Phys. Today* **1993**, *46*, 56. (b) Colvin, V. L.; Goldstein, A. N.; Alivisatos, A. P. *J. Am. Chem. Soc*. **1992**, *114*, 5221. (c) Motte, L.; Billoudet, F.; Douin, J.; Pileni, M. P. *J. Phys. Chem. B* **1997**, *101*, 138. (d) Guo, S.; Popowitz-Biro, R.; Arad, T.; Hodes, G.; Leiserowitz, L.; Lahav, M. *Adv. Mater*. **1998**, *10*, 657.
(11) Fendler, J. H. *Nanoparticles and nanostructured films*: *preparation, characterization and application*; Wiley-VCH: Weinheim, Germany, 1998.
(12) Heitmann, D. J.; Kottaus, P. *Phys. Today* **1993**, *46*, 56.
(13) Kuno, M.; Lee, J. K.; Dabbousi, B. O.; Mikulec, F. V.; Bawendi, M. G. *J. Chem. Phys.* **1997**, *106*, 9869.
(14) Micic, O. I.; Cheong, H. M.; Fu, H.; Zunger, A.; Sprague, J. R.; Mascarenhas, A.; Nozik, A. J. *J. Phys. Chem. B* **1997**, *101*, 4904.
(15) Roberti, T. W.; Cherepy, N. J.; Zhang, J. Z. *J. Chem. Phys.* **1998**, *108*, 2143.
(16) Klimov, V. I.; Schwarz, C. J.; McBranch, D. W.; Leatherdale, C. A.; Bawendi, M. G. *Phys. Rev. B* **1999**, *60*, 2177.
(17) See for example: Wang, Y.; Suna, A.; McHugh, J.; Hilinski, E. F.; Lucas, P. A.; Johnson, R. D. *J. Chem. Phys.* **1990**, *92*, 6927.
(18) Colvin, V. L.; Alivisatos, A. P.; Tobin, J. G. *Phys. Rev. Lett*. **1991**, *66*, 2786.
(19) Nanda, J.; Kuruvilla, B. A.; Sarma, D. D. *Phys. Rev. B* **1999**, *59*, 7473.
(20) Samokhvalov, A.; Berfeld, M.; Lahav, M.; Naaman, R.; Rabani, E. *J. Phys. Chem. B* **2000**, *104*, 8631.
(21) Berfeld, M.; Samokhvalov, A.; Naaman, R.; Lahav, M. *Adv. Mater*. **2001**, *13*, 584.
(22) Nakanishi, T.; Ohtani, B.; Uosaki, K. *Jpn. J. Appl. Phys.* **1999**, *38*, 518.
(23) Naaman, R.; Haran, A.; Nitzan, A.; Evans, D.; Galperin, M. *J. Phys. Chem. B* **1998**, *102*, 3658.
(24) Ueno, N.; Sugita, K. *Phys. Rev.* **1990**, *B42*, 1659. Ueno, N.; Nakahara, H.; Sugita, K.; Fukuda, K. *Thin Solid Films* **1989**, *179*, 161. Maeda, T.; Miyano, K.; Sugita, K.; Ueno, N. *Thin Solid Films* **1989**, *179*, 327.
(25) Nagesha, K.; Sanche, L. *Phys. Rev. Lett.* **1998**, *81*, 5892.
(26) Rei Vilar, M.; Blatter, G.; Pfluger, P.; Heyman, M.; Schott, M. *Europhys. Lett*. **1988**, *5*, 375.
(27) Haran, A.; Naaman, R.; Ashkenasy, G.; Shanzer, A.; Quast, T.; Winter, B.; Hertel, I. V. *Eur. Phys. J. B* **1999**, *8*, 445. Haran, A.; Cohen, H.; Naaman, R. *Superlattices Microstruct.* **2000**, *28*, 279.
(28) Samokhvalov, A.; Gurney, R.; Lahav, M.; Cohen, S.; Cohen, H.; Naaman, R., submitted to *J. Phys. Chem.*
(29) Guo, S.; Konopny, L.; Popovitz-Biro, R.; Cohen, H.; Porteanu, H.; Lifshitz, E.; Lahav, M. *J. Am. Chem. Soc.* **1999**, *121*, 9589. Konopny, L.; Berfeld, M.; Popovitz-Biro, R.; Weissbuch, I.; Leiserowitz, L.; Lahav, M. *Adv. Mater.* **2001**, *13*, 580.
(30) Doron-Mor, I.; Hatzor, A.; Vaskevich, A.; Van der Boom-Moav, T.; Shanzer, A.; Rubinstein, I.; Cohen, H. *Nature* **2000**, *406*, 382.
(31) Heinz, B.; Morgner, H. *Surf. Sci.* **1997**, *372*, 100.
(32) Lingle, R. L., Jr.; Ge, N.-H.; Jordan, R. E.; McNeill, J. D.; Harris, C. B. *Chem. Phys*. **1996**, *205*, 191.
(33) It is assumed that the interaction between the metal states and the states of the QPs is about the same as the interaction between the states of two particles.